© 2018. Published by The Company of Biologists Ltd | Development (2018) 145, dev159699. doi:10.1242/dev.159699

RESEARCH ARTICLE

Prothoracicotropic hormone modulates environmental adaptive plasticity through the control of developmental timing

MaryJane Shimell[1,*,‡], Xueyang Pan[1], Francisco A. Martin[2,3], Arpan C. Ghosh[1], Pierre Leopold[2], Michael B. O'Connor[1] and Nuria M. Romero[2,*,‡]

ABSTRACT

Adult size and fitness are controlled by a combination of genetics and environmental cues. In *Drosophila*, growth is confined to the larval phase and final body size is impacted by the duration of this phase, which is under neuroendocrine control. The neuropeptide prothoracicotropic hormone (PTTH) has been proposed to play a central role in controlling the length of the larval phase through regulation of ecdysone production, a steroid hormone that initiates larval molting and metamorphosis. Here, we test this by examining the consequences of null mutations in the *Ptth* gene for *Drosophila* development. Loss of *Ptth* causes several developmental defects, including a delay in developmental timing, increase in critical weight, loss of coordination between body and imaginal disc growth, and reduced adult survival in suboptimal environmental conditions such as nutritional deprivation or high population density. These defects are caused by a decrease in ecdysone production associated with altered transcription of ecdysone biosynthetic genes. Therefore, the PTTH signal contributes to coordination between environmental cues and the developmental program to ensure individual fitness and survival.

KEY WORDS: *Drosophila* development, Ecdysone, PTTH, Plasticity, Environmental cue

INTRODUCTION

During animal development, tissue growth and physiological integration of tissue function must be timed appropriately to maximize an organism's chances of survival and reproduction. In holometabolous insects, tissue growth is confined to the larval phases of development, which are punctuated by periodic shedding and resynthesis of cuticle (molts) to accommodate an increasing body size. In *Drosophila melanogaster*, embryonic development lasts ∼24 h, as does each of the first and second larval instar stages. During the final, third larval instar, which lasts ∼2-3 days, a great deal of growth occurs and body size becomes fixed in response to various neuroendocrine and hormonal signals that trigger metamorphosis, a process that transforms the larval body into that of the sexually mature adult fly (Mirth and Riddiford, 2007; Nijhout et al., 2014; Rewitz et al., 2013).

Both genetic and environmental factors influence larval growth rate and timing parameters (Danielsen et al., 2013; Di Cara and King-Jones, 2013; Rewitz et al., 2013). For instance, nutritional content of the food source and population density impact many life history traits resulting in numerous trade-offs that must be balanced for optimal survival (Barker and Podger, 1970; May et al., 2015; Miller and Thomas, 1958; Prout and Mcchesney, 1985). In its natural habitat, *D. melanogaster* utilizes rotting fruit, a short-lived food source, as its main dietary resource. As might be expected for such an ephemeral habitat, recent studies have shown that *Drosophila* larvae make nutritional choices that minimize developmental time. This choice impacts other life history traits such as body size, ovariole number (fecundity), viability and life span (Chippindale et al., 1993; Horvath and Kalinka, 2016; Kolss et al., 2009; Mendes and Mirth, 2016; Rodrigues et al., 2015). Despite the importance of balancing various life history traits for robust survival, the genetic mechanisms that adjust insect developmental time in response to various environmental factors are not well understood (Mirth and Shingleton, 2012; Tennessen and Thummel, 2011).

Both molting and metamorphosis require pulsed production and release of the steroid hormone ecdysone (E) from the larval prothoracic gland (PG), and classic ligature and transplantation experiments in Lepidoptera demonstrated that at least one brain-derived factor regulates E production in the PG (Kopec, 1922; Williams, 1952). Subsequent purification of the E-inducing substance from *Bombyx* heads identified prothoracicotropic hormone (PTTH) as a key ecdysteroidogenic inducer (Kawakami et al., 1990). PTTH is a secreted homodimer derived by processing of a precursor pro-protein and is a member of the cystine knot family of growth factors (Noguti et al., 1995). Genetic and biophysical studies have shown that it signals through the receptor tyrosine kinase Torso, which then activates a Ras/Raf/Erk MAP kinase signal transduction cascade (Jenni et al., 2015; Konogami et al., 2016; Rewitz et al., 2009). The targets of this signaling pathway are not fully identified, but are likely to include several of the E biosynthetic enzymes produced in the PG (Gibbens et al., 2011; Niwa et al., 2005).

In *Drosophila*, PTTH is produced by two bilateral neuroendocrine cells located in each brain hemisphere (termed PG neurons, in accordance with their innervation pattern) that project their axons contralaterally to terminate on the PG (McBrayer et al., 2007). These observations suggest that PTTH acts like a neurotransmitter for stimulating ecdysteroidogenesis rather than as a systemic hormone. However, *Drosophila* PTTH has a second role as a modulator of larval light sensitivity. This process involves the release of PTTH into circulation and its systemic delivery to larval light-sensing organs where it enhances larval light avoidance (Yamanaka et al., 2013b).

Genetic ablation or misspecification of the PG neurons revealed that these cells control developmental timing and body size (Ghosh et al., 2010; McBrayer et al., 2007). Loss of the PG neurons resulted

[1]Department of Genetics Cell Biology and Development, University of Minnesota, Minneapolis, MN 55455, USA. [2]University Côte d'Azur, CNRS, Inserm, Institute of Biology Valrose, Parc Valrose, 06108 Nice, France. [3]Cajal Institute, Av Doctor Arce 37, 28002 Madrid, Spain.
*These authors contributed equally to this work

‡Authors for correspondence (oconn033@umn.edu; nromero@unice.fr)

M.J.S., 0000-0003-1378-6017; N.M.R., 0000-0001-6235-1330

Received 20 September 2017; Accepted 12 February 2018

Development (2018) 145, dev159699. doi:10.1242/dev.159699

in substantially delayed pupariation (by 4-6 additional days) and the production of large flies. Delayed pupariation resulted from a belated surge in the 20-hydroxyecdysone (20E) titer during the wandering stage, and both the large body size and developmental delay could be rescued by feeding 20E to third instar larvae. Although these observations suggested that PTTH is likely to be important for proper timing of the normal metamorphic transition, its exact role could not be determined since ablation/misspecification of the PG neurons would eliminate other potential factors, in addition to PTTH, that might influence endocrine activity and the timing of developmental transitions.

To unambiguously determine the role of PTTH in modulating developmental timing in response to various environmental conditions, we produced *Ptth* null mutants using both TALEN and gene replacement technologies. We show that these mutants produce a variable developmental delay that is influenced by both nutrient availability and population density. Careful analysis reveals that mutant animals accumulate mass at wild-type rates and eventually produce larger adults due to a longer growth phase. We find that PTTH function is required throughout the third instar larval stage since the developmental delay extends both the time to reach critical weight – a crucial nutrition-dependent developmental checkpoint (reviewed by Mirth and Riddiford, 2007) – as well as the nutrition-independent terminal growth period (Shingleton et al., 2007). Our experiments also indicate that these phenotypes result from an alteration in the kinetics of E biosynthesis. Furthermore, we demonstrate that PTTH provides animals with better adaptability to challenging environmental conditions (crowding, nutritional limitation). Lastly, manipulation of PG neuron activity demonstrates that PTTH acts in conjunction with another, as yet unknown, factor(s) to properly time larval development. Taken together, our results indicate that PTTH is a central component of a mechanism that coordinates trade-offs in several life history traits in response to environmental inputs such as nutrition and population density.

RESULTS

PTTH controls the onset of metamorphosis, final body size and reproductive capacity

To genetically assess *Ptth* function, we generated three mutants: $Ptth^{Delta}$, $Ptth^{120F2A}$ and $Ptth^{8K1J}$ (Materials and Methods, Fig. 1A). The deletion mutant $Ptth^{Delta}$ removes the start codon and is a protein null, as shown by complete absence of immunostaining signal (Fig. S1A). By contrast, $Ptth^{120F2A}$ and $Ptth^{8K1J}$ are short deletions in the final exon (7 bp and 6 bp, respectively) and yield either a truncated protein or a mature protein that is shortened by two amino acids. The control strain for all $Ptth^{Delta}$ studies was w^{DAH}, while the control for $Ptth^{120F2A}$ and $Ptth^{8K1J}$ was w^{1118} (see Materials and Methods). We determined the ability of the three mutants to undergo metamorphosis by precisely timing the developmental profiles from L1 ecdysis to pupariation. As shown in Fig. 1B, larvae lacking PTTH undergo metamorphosis with a 1 day delay compared with their respective controls. $Ptth^{8K1J}$ exhibits the same 1 day delay as the other *Ptth* mutants, suggesting that all three alleles yield a PTTH product that is non-functional. Additionally, we consider the $Ptth^{120F2A}$ allele to be a genetic null since an identical 1 day delay is observed in transheterozygous ($Ptth^{120F2A}/Ptth^{Delta}$) animals (Fig. S1B). Since *Ptth* mutants show almost no effect on size and timing before third instar (data not shown), this 1 day delay occurs in the third instar larval stage. The developmental delay observed in *Ptth* mutants can be rescued by adding a genomic transgene containing wild-type *Ptth* into the $Ptth^{120F2A}$ background or by using *tub-Gal4* to ubiquitously express a *UAS-Ptth* transgene in the $Ptth^{Delta}$ background (Fig. 1C). These results imply a role for PTTH in precisely timing the transition from juvenile to adult.

Male and female *Ptth* mutant pupae are larger than their respective controls (Fig. 1D,D′), and *Ptth* mutant adults show significant weight increase (Fig. 1E) indicating that the extended larval growth period of these animals increases final adult size. Consistent with these results, *Ptth* mutant larvae gained weight at the same rate as control larvae (Fig. S2A). Accordingly, the size of brains, fat body nuclei and salivary gland nuclei at 24 h after the L2-to-L3 transition was comparable in $Ptth^{Delta}$ mutant and control animals (Fig. S2B-D). Overall, this indicates that PTTH determines final adult body size by controlling the duration of the larval growth period without affecting the bulk rate of mass accumulation in the third instar larva.

Since female body size correlates with ovary size in *Drosophila* (David, 1970; Bergland et al., 2008), we counted ovariole number in $Ptth^{Delta}$ and control females and observed a significant increase in ovariole number (by 8.5%) in the mutant compared with the control (Fig. 1F). This indicates that, by timing the end of the larval period and the onset of metamorphosis, PTTH also influences adult physiology, such as egg production and fecundity.

Ptth mutants exhibit a disrupted imaginal organ growth program

Given the role of E in controlling growth and differentiation of imaginal tissues (Gokhale et al., 2016; Hackney et al., 2012; Herboso et al., 2015; Jaszczak et al., 2016), we examined whether loss of *Ptth* could affect the rate of imaginal disc growth. We measured wing imaginal disc size at 15, 24 and 46 h after L3 ecdysis. As previously found in mutants with reduced E levels (Parker and Shingleton, 2011), $Ptth^{Delta}$ mutant discs grew significantly more slowly than controls (Fig. 2A). We did not observe any difference in cell size between the two genotypes, indicating that lack of PTTH leads to smaller discs with fewer cells (Fig. 2B). However, owing to an extended larval growth period, $Ptth^{Delta}$ wing discs are 14% larger at the onset of metamorphosis and give rise to larger adult wings (Fig. 2C,D). Thus, PTTH has a dual function in regulating both imaginal tissue growth rate and larval growth duration.

PTTH function is required throughout the third instar stage

Drosophila larvae pass through two developmental checkpoints during the final instar: the critical (CW) and the minimal viable weight (MVW) thresholds (Mirth and Riddiford, 2007). In third instar larvae, CW and MVW are reached concomitantly ∼8 h (on rich food) after L2/L3 ecdysis at 0.84 mg/larva (Fig. 3A). It is noteworthy that our determination of CW for wild-type w^{1118} is nearly the same as that reported previously (McBrayer et al., 2007; Mirth et al., 2005) and virtually identical to that determined by Koyama et al. (2014) using the breakpoint method (Stieper et al., 2008). The CW for $Ptth^{120F2A}$ larvae increased to 1.9 mg/larva and occurred ∼20 h after the L2/L3 transition (Fig. 3B). Interestingly, in these mutants, the MVW occurred slightly earlier than the CW and at a lighter weight (1.55-1.69 mg/larva; Fig. 3B). We also determined the length of the terminal growth period (TGP), defined as the time interval that transpires after attainment of CW to when 50% pupariation is achieved (Shingleton et al., 2007). This period was prolonged from 35 h for w^{1118} to 47 h for $Ptth^{120F2A}$ (Fig. 3C). Taken together, these results suggest that 12 h of the 24 h developmental delay in *Ptth* mutants occurs prior to achievement of CW and that the remainder occurs during the TGP.

Development (2018) 145, dev159699. doi:10.1242/dev.159699

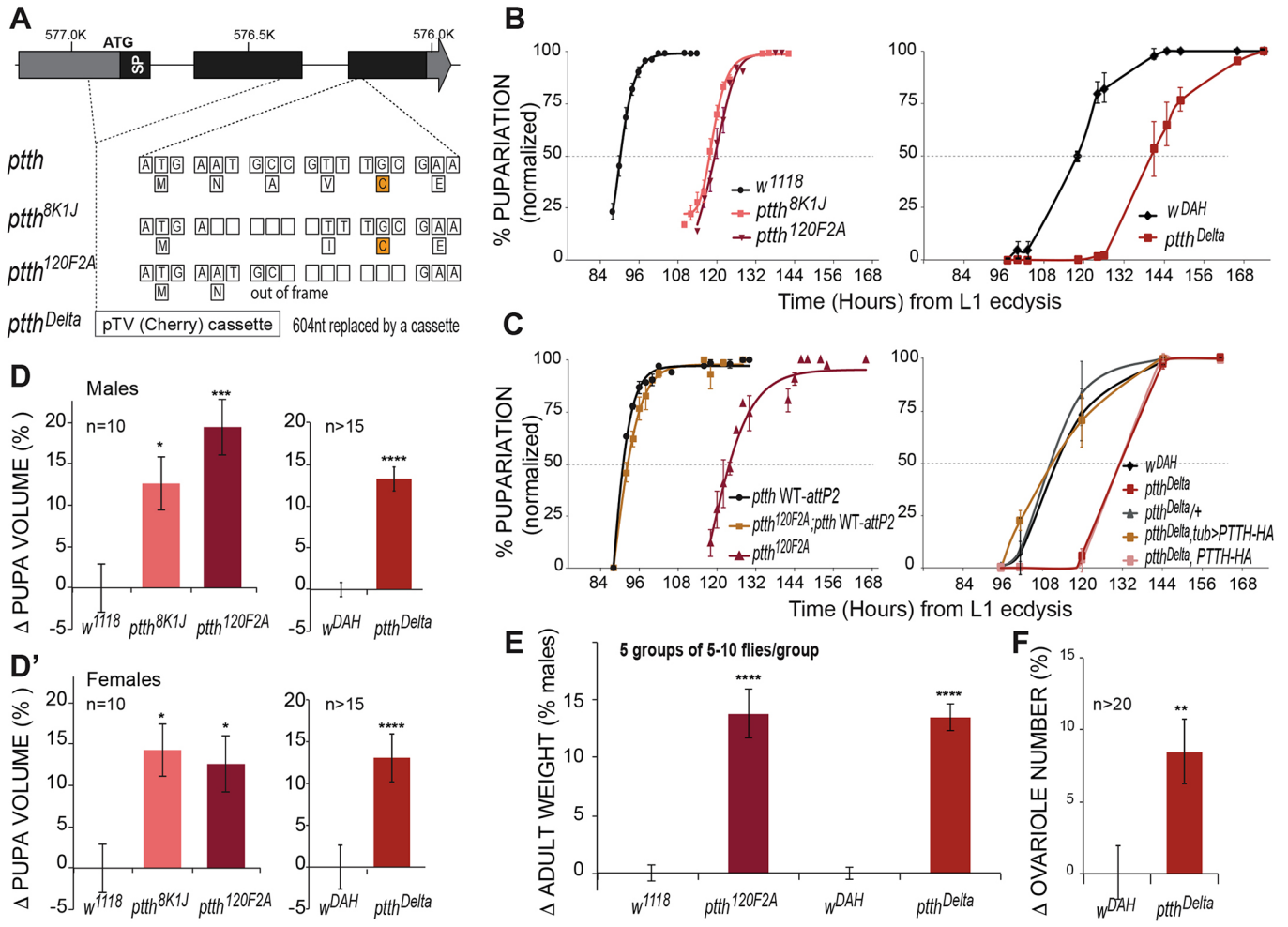

Fig. 1. PTTH controls the onset of metamorphosis, final body size and ovariole number. (A) The *Drosophila Ptth* gene showing nucleotide deletions and amino acid changes of $Ptth^{120F2A}$ and $Ptth^{8K1J}$, as well as the deleted region of $Ptth^{Delta}$. Orange-shaded Cs form part of the cystine knot. SP, signal peptide. (B) Developmental timing curves of w^{1118}, $Ptth^{8K1J}$, $Ptth^{120F2A}$, w^{DAH} and $Ptth^{Delta}$ illustrate a 1 day pupariation delay in all mutant lines. (C) Developmental timing curves demonstrate complete rescue of the timing delay by the *Ptth* WT-*attP2* transgene or by *tub>PTTH-HA* ubiquitous expression as compared with controls. (D,D′) Pupal volumes of male (D) and female (D′) *Ptth* mutants are significantly larger than those of wild-type controls. (E) Adult male *Ptth* mutants are significantly heavier than wild-type controls. (F) The *Ptth* mutant possesses significantly more (8.5%) ovarioles than its wild-type counterpart. Dashed horizontal lines (B,C) denote 50% pupariation. (D-F) *$P \leq 0.05$, **$P \leq 0.01$, ***$P \leq 0.001$, ****$P \leq 0.0001$, unpaired *t*-test. Error bars indicate s.e.m.

Next, we examined the transcriptional timing of three E-responsive genes. Expression of the mid-L3 20E target gene *Sgs3* (Fig. S3A) (Warren et al., 2006) was first detected at 21 h in wild-type larvae and rose rapidly over the next 15 h. In $Ptth^{120F2A}$, *Sgs3* expression was first detected at 24 h (4 h after CW) at a very low level, increased gradually for 1 day (the mid-L3 stage), and then rose abruptly at 48 h. In both cases, white prepupae first appeared 6-8 h after peak *Sgs3* expression (36 h for w^{1118} and 59 h for $Ptth^{120F2A}$). We also examined the expression of *Atet* and *E23*, two putative E transporters that are late L3 20E targets (Hock et al., 2000; Yamanaka et al., 2015) and observed similar delays in their induction (Fig. S3B,C). Taken together, these results indicate that PTTH is likely to control E levels throughout the entire L3 stage.

Ptth mutants exhibit altered kinetics of E production

Since PTTH was originally described as a factor stimulating E production in the PG (Kataoka et al., 1991; Kawakami et al., 1990), we expected that the developmental delay observed in *Ptth* mutants would be the result of altered kinetics in E production. Consistent with this view, feeding 20E to *Ptth* mutant larvae rescued the developmental delay (Fig. S1C). To more directly address the timing of E production, we determined ecdysteroid titers in staged w^{1118} and $Ptth^{120F2A}$ L3 larvae (Fig. 3D). In control larvae, ecdysteroid titers rise to a first plateau of 6-8 pg at the time of CW (8-10 h after the L2-to-L3 transition), followed by a second jump at 18-20 h and then a steady rise to a peak at wandering stage. By contrast, $Ptth^{120F2A}$ mutants have lower basal ecdysteroid titers that reach a titer of ∼6 pg/animal at 20 h after L2/L3 ecdysis, which correlates with the attainment of CW in these mutant larvae. The titer then rises at a slow rate, but eventually reaches a level similar to that of the control by the time of wandering (Fig. 3D). These results demonstrate that PTTH regulates the ecdysteroid production rate during the third instar larval stage to properly time metamorphosis.

We next analyzed the transcriptional timeline of seven E biosynthetic enzymes during the third instar stage of w^{1118} and $Ptth^{120F2A}$ (Fig. S4). The profiles of *nvd* and *spok* were similar, exhibiting a delayed rise in the mutant background, achieving only 50-65% of the w^{1118} peak level just prior to wandering (Fig. S4A,B). *shd* and *phm* displayed a similar slow rise in expression in the *Ptth* mutant background but reached approximately the same peak levels

Development (2018) 145, dev159699. doi:10.1242/dev.159699

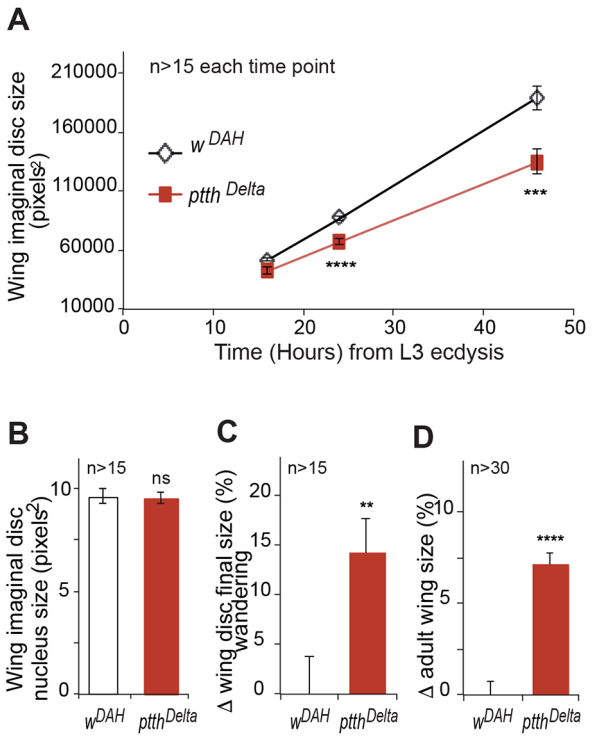

Fig. 2. *Ptth* null mutants exhibit slower imaginal disc growth rate but attain larger disc size. (A) The rate of wing imaginal disc growth of $Ptth^{Delta}$ (red) and w^{DAH} (black) during the third larval instar. (B) At 24 h after the L2/3 transition, there is no difference between wild-type (white) and *Ptth* mutant (red) wing disc nuclear size, suggesting a proliferative difference between wild type and the *Ptth* mutant. (C,D) By the wandering stage, wing imaginal discs of $Ptth^{Delta}$ (red) are larger than those of w^{DAH}, as is the final adult wing size. (A-D) ns, $P>0.05$; $^{**}P\leq0.01$, $^{***}P\leq0.001$, $^{****}P\leq0.0001$, unpaired *t*-test. Error bars indicate s.e.m.

as the control (Fig. S4E,F). By contrast, although expression of *dib* also showed a slow rise, it was induced to less than 50% of wild-type levels (Fig. S4C).

sro and *Cyp6t3* revealed noticeably different transcription profiles compared with the control. In the *Ptth* mutant, *sro* expression peaked in mid-L3 at approximately twice the wild-type level and remained high during the entire extended developmental period before declining in early pupae (Fig. S4G). The expression profile of *Cyp6t3* was drastically reduced on normal food, but remained near normal levels on richer media (Fig. S4D; data not shown). Thus, expression of the E biosynthetic genes is not coordinately regulated in the *Ptth* mutant since transcripts are either upregulated, unchanged, downregulated or dependent on nutrition relative to wild type.

It has previously been suggested that the 'black box' step involving the enzymes Spo/Spok, Sro and Cyp6t3 might be rate-limiting during E biosynthesis (Lafont et al., 2005; Ou et al., 2011; Rewitz et al., 2009). To examine if alterations in the expression profiles of a single enzyme were responsible for the developmental delay, we individually overexpressed some of these genes (*spok*, *Cyp6t3*), as well as *dib* and *nvd* using a PG-specific driver (*p0206-Gal4*) in a *Ptth* mutant background, but observed no rescue of developmental delay induced by *Ptth* loss (Fig. S4H-K). Assuming that all of the UAS constructs provide high-level overexpression, these data suggest that no individual enzyme is rate-limiting as a result of *Ptth* loss. Rather, it is likely that the partial reduction in several enzymes, an as yet unidentified component, or another regulated step is responsible for the slower kinetics of E production and the developmental delay.

PTTH acts autonomously as a trophic factor for PG growth

We have previously suggested that PTTH-expressing neurons provide a growth signal to the PG, since hypomorphic mutations in the *giant* gene induce stochastic unilateral innervation of the PG resulting in an asymmetrically sized PG in which the innervated side is significantly larger than the non-innervated portion of the gland (Ghosh et al., 2010). To determine whether PTTH is the trophic signal, we examined PG nuclear size of innervated and non-innervated PG lobes derived from $Ptth^{120FA2}$, $giant^{E1}$ double-mutant larvae. Whereas the nuclei of innervated lobes were ~33% larger in $giant^{E1}$ PGs, the innervated lobes of $Ptth^{120FA2}$, $giant^{E1}$ double mutants displayed no difference in the size of nuclei compared with non-innervated lobes. Moreover, both innervated and non-innervated lobes of $Ptth^{120F2A}$, $giant^{E1}$ double mutants showed approximately the same nuclear size as the non-innervated PG lobe from $giant^{E1}$ mutants (Fig. 4A,A′). This indicates that loss of *Ptth* leads to the reduced size of the non-innervated PG lobe and demonstrates that PTTH is the trophic signal to the PG.

Next, we inspected glands from larvae in which *Ptth* expression is lost in only one hemisphere of the brain using a Gal4 driver with variegated expression in PG neurons (*NP0394-Gal4*) in combination with *UAS-Ptth-RNAi*. As shown in Fig. 4B, *Ptth* knockdown causes a reduction in lobe as well as nuclear size compared with the contralateral side that has activated PTTH signaling. This confirms that PTTH acts as a PG growth factor. Moreover, PTTH secretion onto one PG lobe cannot compensate for its loss in the other lobe, suggesting that PTTH acts in a local manner.

In most cases, we observed that each PG cell is in contact with at least one varicosity (Fig. S5A). Surprisingly, these varicosity structures co-express PTTH (Fig. 4C′) with synaptic markers such as NC82 (Bruchpilot) (Fig. 4C″, Fig. S5B), Csp (Fig. S5C) and Syb-GFP (Fig. 4C). When populations of PG cells with and without PTTH input are intercalated in the same lobe, the PG cells with PTTH input are larger and express a higher level of Dib than immediate adjacent cells that do not receive PTTH (Fig. 4D,D′). We next generated PG cell clones expressing RNAi targeting the PTTH receptor Torso and observed that PG cells depleted of Torso also contain smaller nuclei (Fig. 4E). These results reveal that synaptically released PTTH acts autonomously through its receptor Torso to control PG cell size.

PTTH is necessary for adaptive response to the environment

A common adaptive strategy that insects use in response to an adverse environment is to adjust the time of larval development at the expense of adult size (Rodrigues et al., 2015). To examine whether PTTH plays a role in adapting individual life history traits to changes in environmental conditions, we evaluated the ability of $Ptth^{Delta}$ larvae to undergo metamorphosis under three diets with different nutrient content depending on their levels of inactivated yeast extract: from 5% (poor) to 17% (normal) and 34% (rich) (see Materials and Methods). When grown on poor food, $Ptth^{Delta}$ larvae were delayed 1 additional day compared with controls (Fig. 5A), with a slight increase in mortality (from 6% to 15%, Fig. 5B). Therefore, concomitant reduction of nutrient signaling and PTTH pathways caused additive effects that could compromise the survival of the organism. We also investigated whether an artificial increase in PTTH levels generated using ubiquitous *tub-Gal4* to drive expression of *UAS-Ptth-HA* could rescue the additional delay caused by growing larvae in low nutrients. As shown in Fig. 5C, PTTH was unable to

Development (2018) 145, dev159699. doi:10.1242/dev.159699

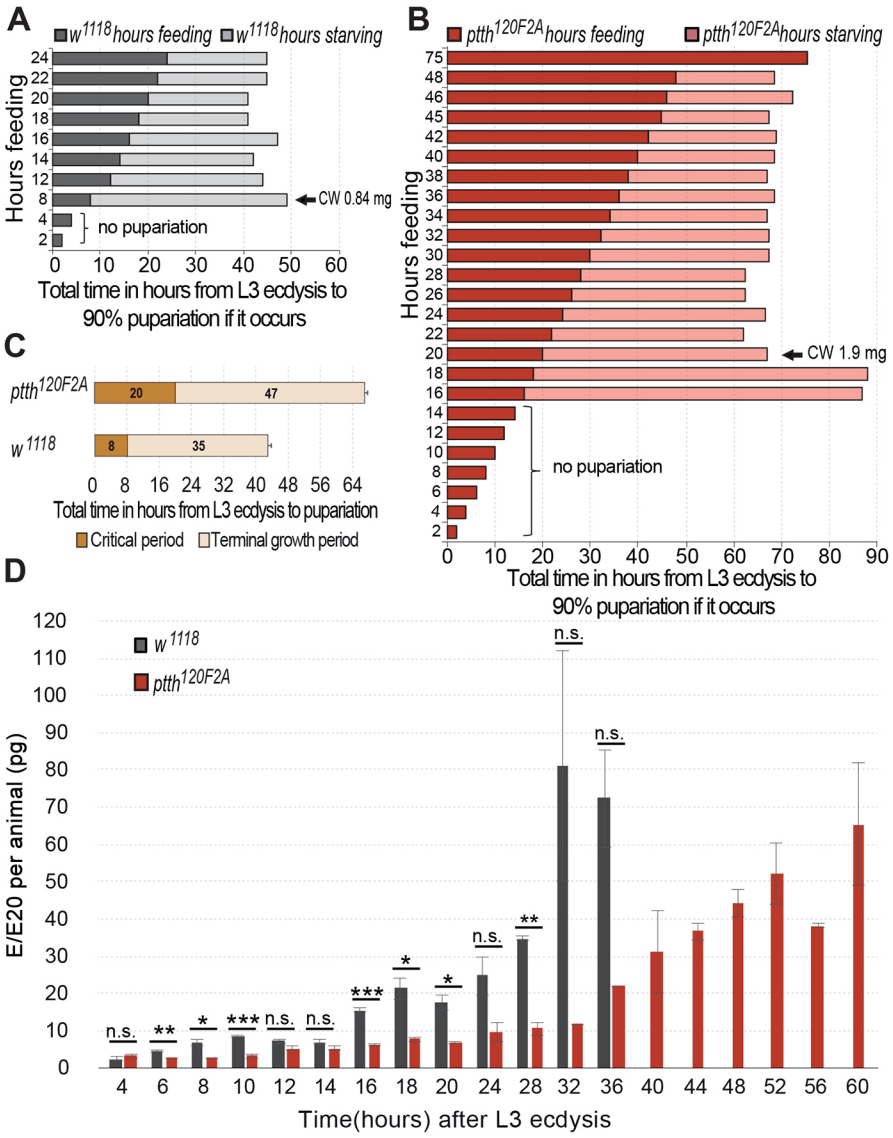

Fig. 3. PTTH sets the critical weight checkpoint and regulates the kinetics of ecdysone production. (A,B) The CW checkpoint of *Ptth*^{120F2A} is about twice that of *w*^{1118} and occurs 12 h later in the third instar stage. The darker bars denote the time spent feeding (value displayed on *y*-axis), while the lighter bars show the time between switching to starvation conditions and achieving 90% pupariation (n=10 feeding larvae per time point). (C) Graphical representation of the critical period and the terminal growth period (average post-CW values ±s.e.m.) along the developmental timeline of *Ptth* mutant and wild type in this trial. (D) Temporal quantitation of E/20E titers of whole third instar larvae. Biological replicates: n=8 for *w*^{1118}, n=2 for *Ptth*^{120F2A}. Shown are average values ±s.e.m. n.s., P>0.05; *P≤0.05, **P≤0.01, ***P≤0.001, unpaired *t*-test.

rescue the developmental delay caused by low nutritional input. Moreover, *Ptth*^{Delta} larvae grown on rich food were still delayed by at least 20 h (Fig. 5A). Thus, PTTH cannot compensate for a low nutritional input and vice versa. These results suggest that several ecdysteroidogenic signals, including PTTH, serotonin (Shimada-Niwa and Niwa, 2014) and nutrient response IIS/Target of Rapamycin (TOR) signaling (Caldwell et al., 2005; Lavalle et al., 2008; Mirth et al., 2005; Walkiewicz and Stern, 2009) are timing metamorphosis in a non-redundant manner and may have additive effects in controlling the adaptive response to the environment.

Next, we tested animal survival in response to a different environmental stress, larval crowding, which is frequently observed in natural populations of *Drosophila* (Bubli et al., 1998). Larval crowding is a multifactorial stressor that, in addition to nutrient restriction, results in inevitable exposure to high concentrations of larval products such as nitrogenous metabolic waste (Joshi et al., 1996a,b; Schering et al., 1984) and pheromones (Mast et al., 2014). Interestingly, a recent report found a strong negative correlation between development time and fitness at high density (Horvath and Kalinka, 2016), meaning that fast developers have higher fitness. To determine if PTTH plays an adaptive role in this condition, L1 larvae were collected and grown at increasing densities in tubes (L1/t) of normal food. As shown in Fig. 6A, *Ptth*^{Delta} mutant and *w*^{DAH} control animals equally survive until adulthood when grown at standard densities (40 L1/t and 150 L1/t). However, survival of *Ptth*^{Delta} animals was drastically reduced at high density (43% at 350 L1/t and 16% at 500 L1/t), compared with control animals (72% at 350 L1/t and 50% at 500 L1/t), with most animals dying at late larval stages (data not shown). This indicates that PTTH is required for optimal survival under crowded as well as nutrient restricted conditions, possibly by fine tuning the duration of larval development. Moreover, the *Ptth*^{Delta} mutant ecloses with a 3-4 day delay in the 500 L1/t condition (Fig. 6B). Therefore, without PTTH, animals cannot properly adapt larval development time and survival to an environmental stress, such as crowding or nutrient restriction.

Because we observed a drastic effect on larval survival in crowded conditions, we tested the effects of this stressor on adult size and ovariole number in *Ptth* mutants and controls. Whereas *w*^{DAH} flies showed strong size adaptation to crowding (73% size reduction in 500 L1/t conditions, see Fig. 6C), *Ptth*^{Delta} mutants were less plastic (52% reduction). This, and the additional delay observed in crowded conditions, mean that *Ptth*^{Delta} adult flies weighed more than 200% of controls at 500 L1/t density, whereas at 40 L1/t the weight difference between *Ptth* mutants and controls was

Development (2018) 145, dev159699. doi:10.1242/dev.159699

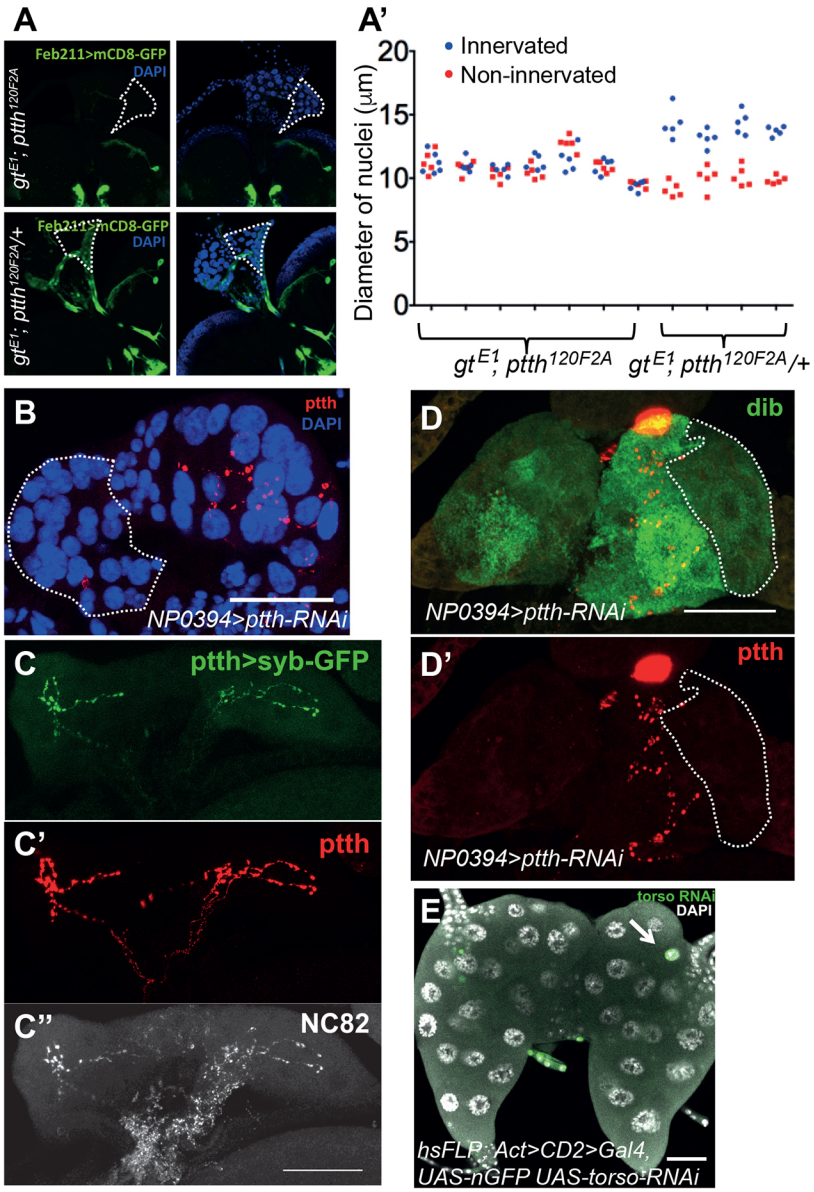

Fig. 4. PTTH acts autonomously as a trophic factor for PG growth. (A,A′) Immunohistochemistry using GFP to mark PG neurons (green) and DAPI staining (blue) to measure PG nuclear size in *Ptth*^{120F2A} (A, top row; A′, left) and wild-type (A, bottom row; A′, right) background illustrates that innervation of one PG lobe (indicated by green staining in the contralateral PG neuron) in the absence of PTTH cannot restore nuclear size to the wild-type level. Dotted line delineates non-innervated brain lobe. (B) Immunohistochemistry with anti-PTTH (red) shows that knockdown of *Ptth* locally in one lobe of the PG (outlined by dotted line; contralateral PG neuron cell bodies not shown) leads to smaller nuclei (blue). (C-C″) Immunohistochemistry showing co-expression of synaptic markers with PTTH in the PG (D,D′) Immunohistochemistry highlights that only PG cells that receive the PTTH signal (red, D′) express high levels of Dib (green, D), whereas neighboring non-innervated cells (outlined with dotted line) do not. (E) Immunohistochemistry shows that knockdown of *torso* in a single PG cell (arrow) marked with anti-GFP (green) leads to smaller nuclei. Scale bars: 50 μm (A-E).

only 20% (Fig. 6C). A similar reduced plasticity in ovariole number was found in *Ptth*^{Delta} females exposed to high population density (Fig. 6D). Overall, these results indicate that PTTH participates in a general mechanism of adaptation to environmental stress, allowing animals to adjust adult size and fecundity to maximize survival.

An additional ecdysteroidogenic signal is produced by PG neurons

The developmental delay that we observe with *Ptth* loss (1 day on rich food) is significantly less than that observed when PG neurons are ablated or misspecified (5-6 days on rich food; see also *Ptth>grim* in Fig. 7B) (Ghosh et al., 2010; McBrayer et al., 2007). In addition, the CW of the *Ptth* mutant (1.9 mg at 20 h after L3 ecdysis, Fig. 3B) is less than that of the PG neuron-ablated animals (2.6 mg at 72 h after L3 ecdysis, Fig. 7G). A simple explanation for these differences would be the existence of an additional ecdysteroidogenic signal(s) produced by the PG neurons. To assess this possibility, we manipulated neuronal activity of PTTH-producing neurons in control or *Ptth*^{120F2A} animals and measured the effect on developmental transitions. When control PG neurons were inactivated by selectively expressing either Kir2.1 (Hodge, 2009) or tetanus toxin (TetxLC) (Popoff and Poulain, 2010), we observed a 17-24 h developmental delay (Fig. 7A), similar to the delay produced by *Ptth* loss. However, inactivation of PG neurons in *Ptth*^{120F2A} larvae induced an additional delay of ∼24 h (Fig. 7B).

In order to activate PG cells, we used the targeted expression of TrpA1 (Hamada et al., 2008) and activated the channel by a temperature shift at various times after the L2/3 transition. As shown in Fig. 7C,E, shifting before or near the time of CW results in the maximal developmental acceleration of ∼17 h. Shifting after CW is still able to accelerate development, but in a graded manner. This is consistent with our data above describing a continuous requirement for PTTH signaling throughout the third instar period. Remarkably, we also see a developmental acceleration of 17 h when TrpA1 is activated in the PG neurons of *Ptth*^{120F2A} (Fig. 7D,F). This acceleration is able to rescue most of the delay caused by *Ptth* loss (Fig. 7F). These data indicate that at least one other factor may be released from the PG neurons to activate pupariation in the absence of PTTH. The existence of this additional signal could explain the

Development (2018) 145, dev159699. doi:10.1242/dev.159699

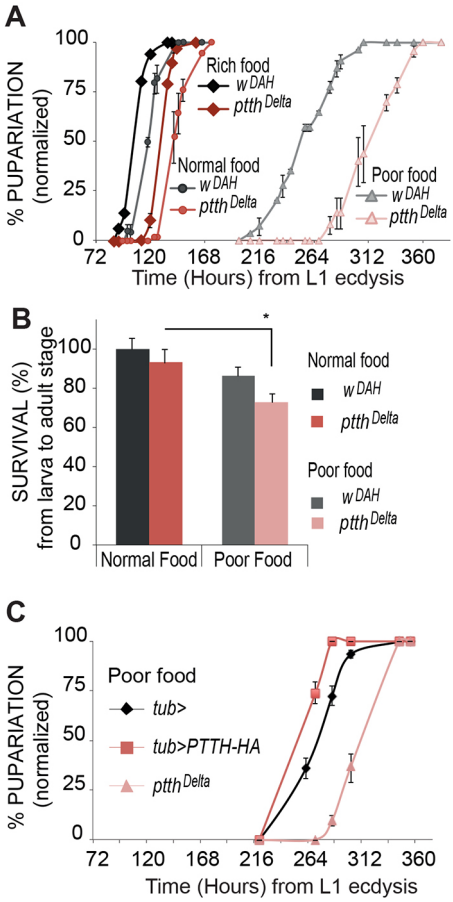

Fig. 5. Effects of nutrition on life history traits. (A,B) Comparison of developmental timing curves of w^{DAH} and $Ptth^{Delta}$ grown on rich, normal or poor food (A) illustrates that whereas $Ptth^{Delta}$ mutants are delayed 1 day when grown in rich or normal food, they are delayed an additional day under poor nutritional conditions and (B) have a slightly elevated rate of mortality. *P≤0.05, unpaired t-test. (C) Developmental timing curves in poor food demonstrate that even if levels of PTTH are elevated by ubiquitous expression using *tub-Gal4* in a wild-type background, timing remains delayed (compare with wild-type expression) from the low nutritional input. Loss-of-function in $Ptth^{Delta}$ on poor food displays the additional 2 day delay. Error bars indicate s.e.m.

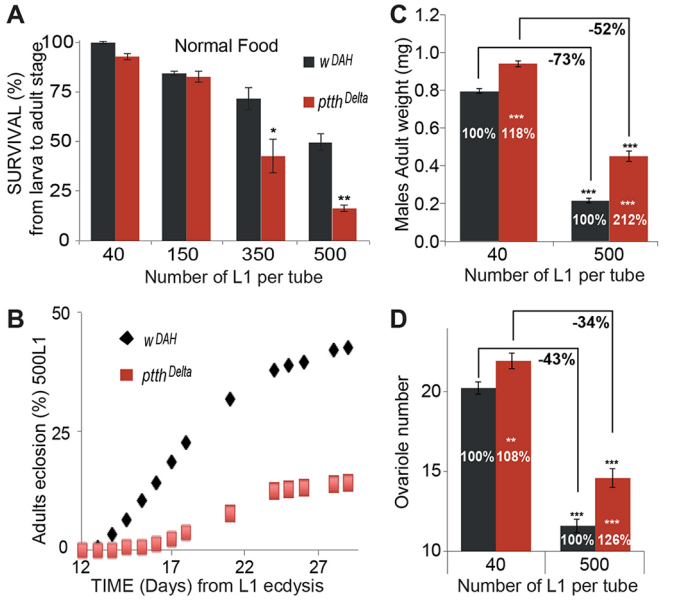

Fig. 6. PTTH plays an adaptive role under larval crowding conditions. (A) Survival graph of w^{DAH} and $Ptth^{Delta}$ highlights decreasing adulthood survival of the mutant as larval density increases. (B) Adult eclosion rate of w^{DAH} and $Ptth^{Delta}$ illustrates decreased survival in crowded larval conditions as well as an additional delay in eclosion timing in the *Ptth* mutant. (C,D) Comparison of w^{DAH} and $Ptth^{Delta}$ in uncrowded (40 L1/t) and crowded (500 L1/t) conditions shows (C) a less severe reduction in mass (values by brackets) and a net increase in weight (values within bars) in $Ptth^{Delta}$; in addition, crowded conditions lead to (D) a less severe reduction in ovariole number (values by brackets) and a net increase in ovariole number (values within bars) in the $Ptth^{Delta}$ mutant. (A,C,D) *P≤0.05, **P≤0.01, ***P≤0.001, unpaired t-test. Error bars indicate s.e.m.

different delays and CWs observed in response to PTTH loss compared with PG neuron ablation.

DISCUSSION

PTTH signaling is a nexus for coordinating environmental input with adaptive plasticity

A central problem that all organisms face is to adjust their development to variation in environmental conditions. This adaptive phenotypic plasticity impacts life history traits, enabling a single genotype to produce an optimized output in the face of fluctuating conditions in its natural habitat. In both vertebrates and invertebrates, neuroendocrine signaling is thought to be a central component of the mechanism that responds to environmental cues to allow phenotypic plasticity (Denver, 1997; Gotthard and Nylin, 1995; Lessells, 2008), but the molecular circuitry remains ill-defined. In this report, we demonstrate that the insect neuropeptide PTTH is a key brain-derived signal that modulates hormone production to alter developmental timing in response to both nutritional cues and population density. In its absence, larvae spend additional time feeding and growing larger, which, in the face of a time-limited food supply such as rotting fruit, is likely to be detrimental to the long-term survival of these individuals. Indeed, recent studies suggest that, given a choice, *Drosophila* larvae regulate their macronutrient uptake (protein versus carbohydrate) to ratios that result in the shortest developmental time (Rodrigues et al., 2015). Short developmental time results in trade-offs with other life history traits such as body size and ovariole number that are maximized by longer developmental intervals and larger bodies (Rodrigues et al., 2015), as we observed for *Ptth* mutants.

Although we do not yet know all the various inputs that PG neurons integrate, their extensive dendritic arbors (Ghosh et al., 2010; McBrayer et al., 2007) suggest that they are capable of processing a multitude of extrinsic and intrinsic signals. For example, Ilp8 (Dilp8), an imaginal disc damage-induced signal, is received by a set of LGR3-positive neurons that in turn contact PTTH dendrites to reduce PTTH production or release to prolong larval development and thereby facilitate damage repair (Colombani et al., 2015; Garelli et al., 2015; Jaszczak et al., 2016; Vallejo et al., 2015). Likewise, in larval and maturing pupal brains, a subset of central circadian clock neuron terminals are in close proximity to the PG neuron dendritic field, and recent studies have shown that PTTH helps coordinate the activity of the central brain clock with the peripheral clock found in the PG (Selcho et al., 2017). This circuit ensures circadian rhythmicity during pupal development, which both influences the timing of pupal development and the observed rhythmicity of adult eclosion that may aid in reproductive success (Kouser et al., 2013). PTTH signaling has also been shown to enhance larval light avoidance at

Development (2018) 145, dev159699. doi:10.1242/dev.159699

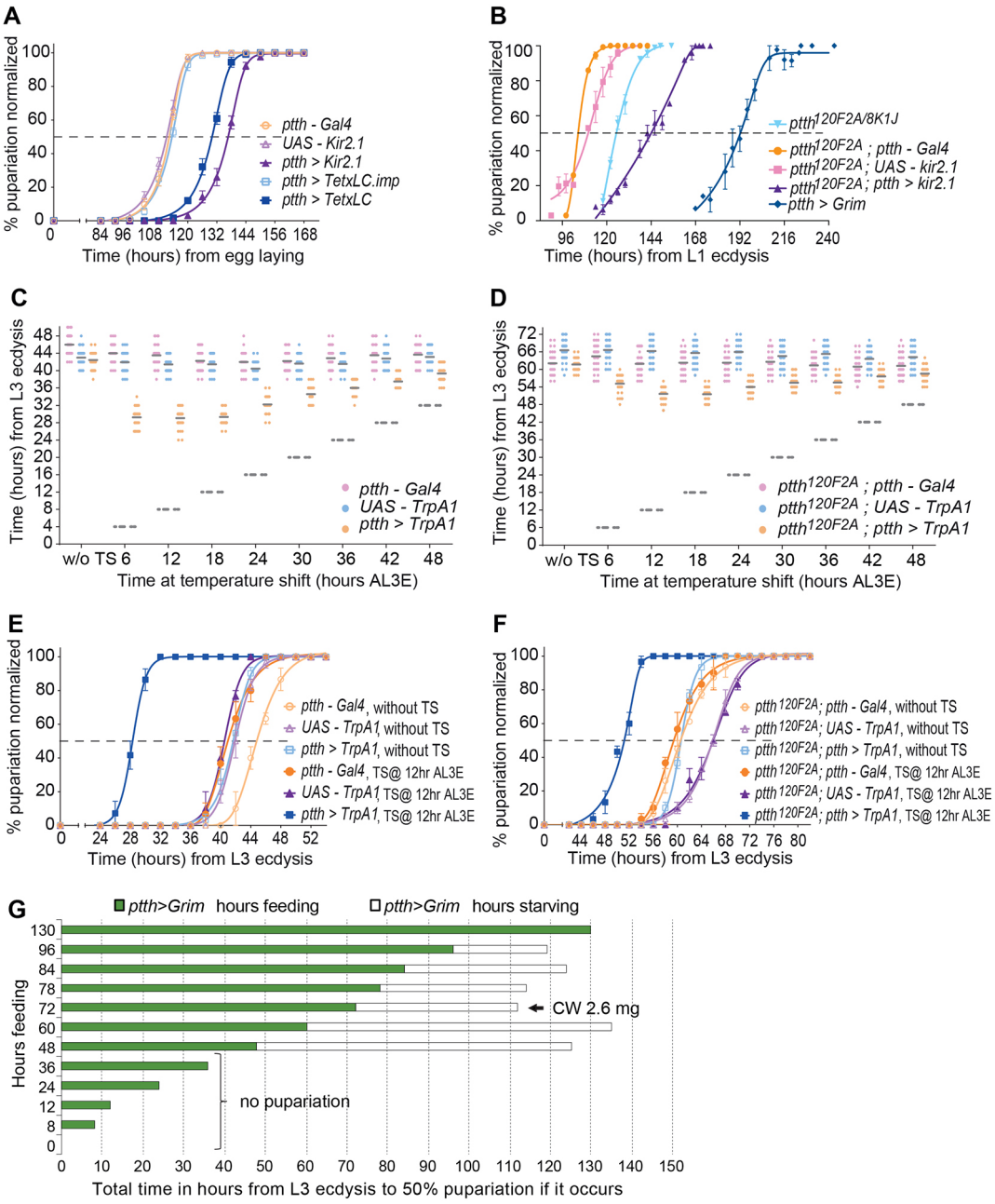

Fig. 7. Electrical manipulation in PG neurons suggests additional ecdysteroidogenic inputs. (A) Inactivation of electrical activity in PG neurons by TetxLC or Kir2.1 results in a timing delay (purple and dark blue) that relies on active toxin (light blue; imp is inactive). Yellow and lilac curves are transgene controls. (B) Inactivation of electrical activity in the PG neurons further delays timing in the *Ptth* mutant background (compare light blue and purple). However, the additive delay is not as great as that associated with PG neuron ablation (dark blue). Yellow and pink curves are transgene controls. (C,D) Temperature shifts at 6 h intervals (dashed lines) and plot of pupariation after L3 ecdysis (AL3E). TrpA1 activation (yellow) is best at 12 h (timing curves shown in E and F). Transgene controls are in pink and light blue. (E,F) Developmental timing curves illustrate acceleration in the 50% pupation time when the TrpA1 calcium channel is activated by temperature shift (TS) in PG neurons (dark blue) in both wild-type and *Ptth* mutant backgrounds. The control without TS is light blue. Yellow, lilac, orange and purple curves are transgene controls. (A,B,E,F) Error bars indicate s.e.m. (G) The CW checkpoint of *Ptth>grim* is about 1.3-fold and 2-fold those of $Ptth^{120F2A}$ and w^{1118} and occurs 52 and 64 h later, respectively. The green bars denote the time spent feeding (value displayed on *y*-axis), while the white bars show the time between switching to starving conditions and achieving 90% pupariation. *n*=10 feeding larvae per time point.

the time of pupation via an E-independent mechanism (Yamanaka et al., 2013a). This process ensures pupation in dark environments, which is likely to aid in pupal survival by reducing dehydration and predation. These examples suggest that the PG neurons, and PTTH signaling in particular, facilitate coordination of developmental processes with environmental conditions to maximize species fitness.

PTTH signaling, critical weight determination and E production kinetics

In holometabolous insects, feeding during the larval stages is especially important for their developmental program since they must accumulate sufficient energy reserves to fuel metamorphosis during the non-feeding pupal stage. As a consequence, various nutritional checkpoints such as CW and MVW have evolved to

Development (2018) 145, dev159699. doi:10.1242/dev.159699

ensure that larvae do not enter metamorphosis before sufficient fuel has been stored. Two studies have put forward different mechanisms for determining CW. In the first, the process of larval molting is proposed to produce a transient starvation state leading to nuclear accumulation of a FoxO-USP complex that inhibits E production until sufficient feeding relieves this constraint and CW is achieved (Koyama et al., 2014). In the second paradigm, nutrient-dependent TOR signaling in the PG is thought to regulate endocycle entry, and DNA copy number is found to correlate with attainment of CW (Ohhara et al., 2017). Our examination of *Ptth* mutants clearly demonstrates that PTTH signaling also contributes to setting the CW checkpoint. All three processes share a common feature in that they affect the rate of basal E production, providing support for the notion that CW represents the attainment of a minimal threshold level of E that enables nutrient-independent completion of larval development and commencement of metamorphosis (Rewitz et al., 2013). It is interesting that the low basal E titer caused by *Ptth* loss does not influence larval growth rate, whereas lower basal levels of E produced by other methods have been reported to enhance larval growth rate (Boulan et al., 2013; Colombani et al., 2005; Moeller et al., 2017). We are presently investigating the mechanism responsible for these differences.

Whether and how these three molecular mechanisms intersect remains to be determined, but it is interesting to note that in our present study we demonstrated a role for PTTH in regulating nuclear size. Thus, PTTH signaling might modulate E production in conjunction with TOR by determining the number of DNA templates available for transcription of E biosynthetic enzymes. Alternatively, PTTH might act more directly to influence transcriptional control of E biosynthetic components. Numerous transcription factors, including EcR, Mld, Usp, FoxO, Br, Ftz-f1, HR4, Vvl and Ouija board (Danielsen et al., 2014; Komura-Kawa et al., 2015; Koyama et al., 2014; Moeller et al., 2013; Ou et al., 2011; Parvy et al., 2005) have been implicated in transcriptional regulation of one or more E biosynthetic enzymes, although none has been shown to be a direct target of Rolled (Erk) phosphorylation, the major downstream mediator of PTTH signaling. One factor of particular interest, however, is the nuclear receptor HR4, since it has been shown that knockdown of its expression in the PG accelerates development, while overexpression retards development (Ou et al., 2011). Furthermore, during the first half of the third instar stage, HR4 cycles in and out of the nucleus with a periodicity that depends on Ras/Erk signaling. The proposed mechanism posits that HR4 negatively regulates one or more E biosynthetic genes, including *Cyp6t3*, and that periodic PTTH signals enable the production of transient small E pulses, each of which might represent passage through a specific developmental checkpoint that controls timing of metamorphosis (Ou et al., 2011; Rewitz and O'Connor, 2011; Rewitz et al., 2013). Although this mechanism is an attractive possibility, we find no rescue of developmental timing when certain biosynthetic enzyme genes, including *Cyp6t3*, are individually overexpressed. These observations indicate that either there is an as yet unidentified PTTH-regulated rate-limiting component, or that it is the combined reduction in several enzymes that results in slower E production. Lastly, in Lepidoptera, PTTH has been shown to stimulate translation as well as transcription and this might also come into play when considering how a slow rise in E titer is produced (Keightley et al., 1990; Kulesza et al., 1994; Rybczynski and Gilbert, 1995).

Autonomy versus non-autonomy of PTTH signaling

One of the more unexpected findings of this study is that *Drosophila* PTTH appears to act autonomously for regulating E biosynthesis within the PG, whereas a previous study demonstrated that PTTH in the hemolymph acts non-autonomously, and in a Torso-dependent manner, to regulate larval light avoidance (Yamanaka et al., 2013b). In addition, a recent study showed that Torso expression in the fat body is required for proper insulin signaling and body size control although the ligand involved was not identified (Jun et al., 2016). Since PTTH reaches the PG through the circulatory system in Lepidoptera, it is unlikely that there is an intrinsic functional need to regulate E biosynthesis through direct innervation of the PG, and indeed we found that overexpression of PTTH in the fat body was able to rescue the developmental delay and body size phenotypes of *Ptth* null mutants (data not shown). This apparent dichotomy with respect to autonomous and non-autonomous requirements in different tissues might be explained by the unusual biophysical features of Torso, which binds PTTH asymmetrically resulting in anti-cooperativity (Jenni et al., 2015). Thus, receptor levels determine the nature of the signal output: high receptor levels stimulate a transient burst of enhanced signal, whereas low receptor levels produce a low amplitude, sustained signal. In addition, high receptor levels may facilitate intermolecular disulfide bond formation between Torso monomers within the transmembrane domain and thereby stabilize a preformed dimeric receptor that is primed for activation by ligand binding (Konogami et al., 2016). Perhaps innervation of the gland by PG neurons facilitates clustering of receptors at the synapses, stimulating production of preformed receptor dimers near the PTTH release sites and resulting in a high-level signal in the PG cells that is necessary for rapid induction of E biosynthetic enzymes. By contrast, the non-autonomous effect of PTTH on Bolwig's organ and class IV multidendritic neurons might result from low receptor concentrations leading to the sustained low-level signal needed to modulate light avoidance. It is interesting to note in this regard that we cannot detect endogenous Torso protein by immunolocalization in Bolwig's organ or class IV multidendritic neurons, but can readily detect it in PG cells, consistent with the idea that receptor levels may influence the type of signal produced by PTTH in different tissues.

An alternative possibility is that two synergistic signals, one of which is localized in the PG, are required to produce rapid induction of E biosynthetic gene transcription in the PG, but two signals are not required for light avoidance. We provide evidence that at least one other signal from the PG neurons is essential for proper timing of E production. Local loss of this signal in cells lacking a varicosity could be sufficient to prevent high-level induction of E biosynthetic enzymes in those cells, while release of PTTH from remaining varicosities could provide sufficient systemic levels of PTTH to stimulate light avoidance. It is interesting to note with respect to the two-signal model that, in a tissue culture assay system, Torso activation can be stimulated by the synergistic interaction of Trunk, a second Torso ligand involved in the specification of terminal embryonic cell fates, and Tsl, the product of the *torso-like* locus (Amarnath et al., 2017).

Additional timing signals produced by PG neurons

Although the data presented here provide strong evidence that PTTH is a key environmentally responsive developmental timing signal in *Drosophila*, our manipulation of PG neuron activity, coupled with previously reported ablation studies (Ghosh et al., 2010; McBrayer et al., 2007), clearly suggest the presence of at least one additional timing factor, the release of which is activity dependent. Whether this factor also signals through Torso or another receptor is unresolved, but it is interesting to note that spätzle-like proteins show some structural features common to both PTTH and Trunk, the two known Torso ligands (Casanova et al., 1995). The presence of multiple timing signals is perhaps not

Development (2018) 145, dev159699. doi:10.1242/dev.159699

surprising since redundancy is likely to provide both robustness to the circuit and flexibility for output responses. Recent characterization of *Ptth* mutants in *Bombyx* also showed alterations in developmental timing during larval stages (Uchibori-Asano et al., 2017). However, there was much more variability in the timing delay phenotype, as well as significantly enhanced lethality, compared with what we observe in *Drosophila*, perhaps indicating that alternative signals are either not present or less effective in compensating for *Ptth* loss in *Bombyx*.

MATERIALS AND METHODS

TALEN-directed mutagenesis

Plasmids TAL248NN and TAL249NN (in the pT3TS-delta152, +63 backbone) were digested with *Ecl*136II, and 1 µg was transcribed using the T3 mMessage mMachine Kit (Ambion). The 5′-capped mRNAs were phenol-chloroform extracted and precipitated with isopropanol. These left and right *Ptth* TALEN monomers were dissolved in 30 µl 0.1× PBS (DEPC treated) and mixed to make a 30 µl solution with each mRNA at a final concentration of 400 µg/ml in 0.1× PBS. An aliquot was injected into w^{1118} embryos (Duke Injection Services) and individual G0 adults were crossed to balancer line sna^{Sco}/CyO* (BDSC #3198). Once larva were observed in the vial, the G0 fly was removed and frozen at −80°C for subsequent single-fly DNA extraction with squishing buffer (Gloor et al., 1993). Genomic DNA from 75 fertile G0 flies was analyzed by PCR with primers PTTH TAL 01F and PTTH TAL 03R (Table S1) incorporating the LightCycler 480 High Resolution Melting Master (Roche) and using the Tm calling program. Five mosaic G0 lines were selected based on an altered Tm peak: either wider, displaying a shoulder, or the presence of two Tm peaks. Ten to fifteen individual balanced F1 males from the mosaic candidates were backcrossed to w*;sna^{Sco}/Cyo* females and then self-crossed to obtain homozygous stocks. These homozygous stocks were again analyzed by Tm calling and the region of interest sequenced. Subsequent analyses used w^{1118} as the control to the $Ptth^{120F2A}$ and $Ptth^{8K1J}$ mutants since that was the line originally injected and so should adequately serve as a control.

Two distinct lesions were found at the targeted *Ptth* site, and no additional changes were observed in these lines when the complete gene was sequenced. The lesions identified comprise: (1) a 7 bp deletion (ΔCGTTTGC between nucleotides 465 and 471 of the PTTH-RF coding sequence) in line $Ptth^{120F2A}$; and (2) a 6 bp deletion (ΔATGCCG between nucleotides 461 and 466 of the PTTH-RF coding sequence) in line $Ptth^{8K1J}$. The $Ptth^{120F2A}$ allele generated a frameshift distal to N154 of PTTH-PR that continued out of frame for 24 amino acids before reaching a stop codon. This mutation removed much of the predicted mature ligand portion of PTTH. The 6 bp deletion found in line $Ptth^{8K1J}$ leads to a deletion of N154 and A155 and a V156I substitution (Fig. 1A). A third allele, $Ptth^{8M9A}$, which deleted 5 bp (ΔCGTTT) between nucleotides 465 and 469 of the PTTH-RF coding sequence, was not used in this work.

Accelerated homologous recombination mutagenesis

To generate the $Ptth^{Delta}$ mutant, the accelerated homologous recombination technique was used as described (Baena-Lopez et al., 2013). Two homology arms were amplified from genomic DNA using the primers listed in Table S1, which incorporate *Not*I or *Bgl*II restriction sites for cloning. The resulting PCR products were digested and cloned into pTV-Cherry vector (2.7 kb corresponding to the 5′ arm with *Not*I and 2.3 kb for the 3′ arm with *Bgl*II). This *Ptth* targeting vector, containing the appropriate homology arms, was introduced at random genomic locations by P-element-mediated transformation (BestGene). Transformants (not necessarily mapped or homozygosed) were crossed to *hs-FLP, hs-I-SceI* flies (BDSC #25679) and the resulting larvae were heat shocked at 48 h and 72 h after egg laying for 1 h at 37°C. Approximately 200 adult females with mottled red eyes (indicating the presence of the targeting vector and the transgene carrying hs-FLP and hs-I-SceI) were crossed to *ubiquitin-Gal4[3×P3-GFP]* males and the progeny screened for the presence of red eyes. The *ubiquitin-Gal4[3×P3-GFP]* transgene was subsequently removed by selecting against the presence of GFP in the ocelli. Red-eyed flies resulting from these crosses were subjected to PCR with primers PTTH forward and reverse (Table S1). One line was confirmed to be a *Ptth* null homologous recombinant, referred to herein as $Ptth^{Delta}$. Sequencing results confirmed a deletion of 604 bp in the $Ptth^{Delta}$ allele that included the putative ATG and signal peptide (Fig. 1A).

The $Ptth^{Delta}$ allele was backcrossed into the w^{DAH} standardized genetic background for at least ten generations before any experimental procedures. Thus, we used w^{DAH} as the correct background control for $Ptth^{Delta}$.

Molecular biology and production of transgenic lines

D. melanogaster release 6 (FlyBase Consortium) was used to define the DNA, RNA and amino acid coordinates of *Ptth*. Three start sites are identified in FlyBase, and we used the cDNA identified as G.

The genomic fragment of HA-tagged PTTH from pMBO2318 (McBrayer et al., 2007) was excised as a *Not*I-*Eco*RI fragment and placed in a *pattB* vector (pattB-QF-sv40, Addgene #24367) which was digested with *Not*I and *Eco*RI in order to drop out the QF fragment. This plasmid, pMBO2604, was inserted into the *attP2* site of $y^1\ w^{67c23}$; *P[CaryP]attP2* (BDSC #8622) by injection (GenetiVision) and *phiC31* integration. The transformant line was designated *Ptth* WT-*attP2-2A3*. The *spok>Gal4* line was made by inserting a 1.4 kb upstream fragment of *spok* (Komura-Kawa et al., 2015) into the Pelican-Gal4 vector (from M.B.O.'s lab.). Transgenic line *spok-Gal4* 1L3 was derived after injection into w^{1118}.

Fly stocks, stock building and food

Animals were reared at 25°C on a variation of standard cornmeal food (CMF, BDSC), in which brewer's yeast was substituted for baker's yeast and Tegosept was added for mold control. Live baker's yeast granules were shaken liberally onto the surface. Some timing experiments were performed on 'normal' fly food, which contains per liter: 17 g inactivated yeast powder, 83 g corn flour, 10 g agar and 4.6 g Nipagin; for 'rich' or 'poor' food, the amount of inactivated yeast powder was adjusted to 34 g/l or 5 g/l, respectively.

The following fly stocks were used: *P0206-Gal4* (Colombani et al., 2005), *UAS-spok 4A2* (Komura-Kawa et al., 2015), *UAS-dib 20A2* (*Not*I-*Asp*718I *dib* cDNA in pUAST), *UAS-nvd* (Yoshiyama et al., 2006), *spok-Gal4 1L3* and *UAS-Cyp6t3* (Ou et al., 2011), *fb-Gal4* (Tom Neufeld, University of Minnesota, USA), *UAS-Ptth HA 96L3* (McBrayer et al., 2007), gt^{E1};*UAS-GFP;*Feb^{211}*-Gal4, UAS-mCD8-GFP* (Siegmund and Korge, 2001), *Ptth-Gal4 45A3, 117bA3* (McBrayer et al., 2007), *Ptth-Gal4 45A3, 117bA3; UAS-grim* (McBrayer et al., 2007), *UAS-TrpA1/TM6B, Tb* (BDSC #26264), *UAS-Kir2.1* on the 3rd chromosome (BDSC #6595), *UAS-TetxLC* on the 3rd chromosome (BDSC #28997), *UAS-TetxLC.IMP* on the 3rd chomosome (BDSC #28841), *UAS-dORKΔC* on the 3rd chromosome (BDSC #6586), *NP0394-Gal4* [*Drosophila* Genetic Resource Center (DGRC) Kyoto, Japan #103604], *UAS-Ptth-RNAi* (Vienna *Drosophila* Resource Center (VDRC) #102043], $UAS\text{-}torso\text{-}RNAi_{GD}$ (VDRC #36280), *UAS-Synaptobrevin-GFP* (BDSC #60677) and *Ay-Gal4 (act-FRT-stop-FRT-Gal4)* (BDSC #3953). Recombinant or combination stocks were made using standard genetic methods.

Developmental timing curves

All developmental timing experiments were performed at 25°C in 12 h light/dark cycle conditions. One- to four-hour time collections of embryos laid on apple juice plus yeast paste plates were aged for 20 h, at which point freshly ecdysing L1 larvae were transferred to vials. Each vial contained 30, 40, 150, 350 or 500 L1 larvae. The time and date of pupariation were scored every 1-5 h during the light cycle and the time in hours from L1 ecdysis to puparium formation was determined using the time duration calculator (www.timeanddate.com). Data from four vials were compiled and ordered by progressive pupariation time and cumulative percentage pupariation and subsequently analyzed in GraphPad Prism using non-linear regression curve fit or in Microsoft Excel.

Measurements of pupal volume and adult mass

Male and female pupae were photographed and measured with ImageJ. Pupal length was measured along the medial line between anterior and posterior, not including the anterior and posterior spiracles. Pupal width was measured along the axial line. Pupal volume was determined using the formula for a prolate spheroid: $(\pi/6)W^2\times L$, where W is width and L is

Development (2018) 145, dev159699. doi:10.1242/dev.159699

length. Sexed adults were weighed in groups of three to five flies or individually using a Mettler Toledo XP26 microbalance.

Immunohistochemistry of larval tissues

Tissues dissected from larvae in 1× PBS (137 mM NaCl, 2.7 mM KCl, 4.3 mM Na_2HPO_4, 1.47 mM KH_2PO_4, pH 8) at the indicated hours after egg deposition were fixed in 4% formaldehyde (Sigma) in PBS for 20 min at room temperature, washed in PBS containing 0.1% Triton X-100 (PBT), blocked for 2 h in PBT containing 10% FBS (PBS-TF), and incubated overnight with primary antibodies at 4°C. The next day, tissues were washed, blocked in PBS-TF, and incubated with secondary antibodies for 2 h at room temperature. After washing, tissues were mounted in Vectashield containing DAPI (Vector Labs) for staining of DNA. Fluorescence images were acquired using a Leica SP5 DS (20× and 40× objectives) and processed using Adobe Photoshop CS5 or ImageJ.

Antibodies

Primary antibodies were anti-PTTH (guinea pig, 1:200; P.L.), anti-NC82 (mouse hybridoma, 1:50; DSHB), anti-Dib [rabbit, 1:500; Parvy et al. (2005)] and anti-GFP (rabbit polyclonal, 1:500; Abcam). Secondary antibodies were Alexa Fluor 555 goat anti-guinea pig, Alexa Fluor 488 sheep anti-rabbit, AlexaFluor 488 donkey anti-rabbit (1:500; Abcam) and Cy3 sheep anti-mouse (1:200; Jackson ImmunoResearch).

Wing disc analyses: growth rate and nuclear size

Four-hour egg collections were performed on agar plates, and after 20 h L1 larvae were collected and reared at 40 animals per tube at 25°C. Larvae that ecdysed from L2 to L3 over a 2 h period were transferred onto new food plates and allowed to feed until they reached the appropriate age. After immunohistochemistry of larval tissues, the image of wing discs was acquired using a Leica SP5 DS, and the disc and nucleus area were measured using ImageJ.

Wing size measurement

L1 larvae were collected 24 h after egg deposition (4 h egg collections) and reared at 40 animals per tube at 25°C. Adult flies of the appropriate genotype were collected and stored in ethanol and mounted in a Euparal solution (ROTH). Images of dissected wings were acquired using a Leica MZ16 FA fluorescence stereomicroscope and DFC 490 digital camera. Wing areas were measured using ImageJ.

Adult ovariole number

Newly eclosed flies were maintained in vials on standard food until the time of dissection (3-4 days after eclosion). Ovaries were dissected in cold PBS, and ovarioles were teased apart and counted under a dissecting microscope.

Determination of critical weight

A variation of published methods (McBrayer et al., 2007; Mirth et al., 2005) was used. Larvae were raised at 25°C in continuous light conditions. Newly ecdysed L1 larvae, as described above, were transferred at intervals to CMF in 35 mm diameter plates and aged for 48 h. Freshly ecdysed L3 larvae were transferred to a new CMF plate at 1 h intervals at a density of less than 30 L3 larvae per plate, and timing initiated. Every 2 h starting at L3 ecdysis (T0) and continuing until 24 h for w^{1118} and 48 h for $Ptth^{120F2A}$, ten feeding larvae were removed, individually weighed and placed in starvation medium [1.5% Bacto Agar (BD Diagnostics) in water]. Puparium formation was quantitated and timed, as well as eclosion rates. The critical period was defined as the number of hours after starvation when ≥90% of the larvae pupariated and did so without a delay. The CW was the average weight of those ten larvae at the critical time.

Rescue by 20-hydroxyecdysone feeding

Thirty freshly ecdysed $Ptth^{120F2A}$ L3 larvae, grown at 25°C under 12 h light/dark conditions, were washed with water and transferred to a small CMF plate for additional aging. After 20 h, larvae were washed and transferred to a vial supplemented with either 20-hydroxyecdysone (Cayman Chemical; dissolved in 95% ethanol, final concentration 0.2 mg/ml) or 95% ethanol (same volume as 20-HE). The control w^{1118} larvae were directly transferred to vials upon L3 ecdysis. Once seeded with L3 larvae, the vials were returned to 25°C under 12 h light/dark and monitored, as well as timed, for pupariation.

PG neuron innervation studies

To show that PTTH is the trophic signal to the PG, females of genotype gt^{E1}/*FM, act-GFP; *$Ptth^{120F2A}$*/CyO, act-GFP* were crossed to $Ptth^{120F2A}$*; *Feb^{211}*-Gal4, UAS-mCD8-GFP* males. CNS plus RG complexes from GFP-negative wandering larvae were dissected, fixed and mounted. About 25% of animals had asymmetric innervation. For the same purpose, females of the variegated driver *NP0394-Gal4* were crossed to *UAS-Ptth-RNAi* and the offspring larvae were grown on food containing per liter: 8.5 g inactivated yeast powder, 83 g corn flour, 10 g agar and 4.6 g Nipagin. CNS plus RG complexes were dissected, fixed and stained with anti-PTTH antibody. About 15% of animals had asymmetric *Ptth* silencing.

Torso RNAi Flp-out clones

Mitotic clones marked by GFP were generated using *hsFLP; Act>CD2>Gal4, UAS-nGFP* in combination with *UAS-torso-RNAi*. Clonal induction was performed for 5 min at 37°C in the second instar.

PG neuron activation by TrpA1

Larvae of the indicated genotypes were first synchronized at L2/L3 molting, and then vials of 25-30 larvae were further reared at 25°C. Vials were transferred to 29°C at progressive times to activate the TrpA1-expressing neurons. Pupariation was monitored by counting the number of pupae at consecutive time points.

Raising L3 larvae for timed sample collections

Timed samples were raised at 25°C under continuous light. Forty newly ecdysed L1 larvae, precisely timed on apple juice collection plates, were transferred at 1 h intervals to 35 mm diameter plates containing CMF with surface granules of live baker's yeast. Larvae continued to develop for ∼48 h and were then monitored for morphological features characteristic of ecdysis to the third instar stage. These freshly ecdysed L3 larvae were transferred to a fresh food plate, and timing of L3 age in hours commenced. For qRT-PCR, larvae of defined ages were removed from the food, washed in DEPC-treated water, homogenized in Trizol (Invitrogen), and stored at −80°C. For E titers, larvae of defined ages were removed from the food, washed twice in water, dried on a Kimwipe, weighed in bulk for biological replicates, and stored at −80°C.

qRT-PCR

Total RNA was purified from Trizol, transcript RNA was isolated using the RNeasy Mini Kit (Qiagen), and reverse transcribed with the SuperScript III First-Strand Synthesis Kit (Invitrogen). qRT-PCR reactions used LightCycler 480 SYBR Green I Master Mix on a LightCycler 480 instrument (Roche). Primers are listed in Table S1. All reactions were performed in duplicate. Expression (arbitrary units) was determined relative to *RpL23* using the formula $(2^{-\Delta Cp})\times 100{,}000$ (or a factor that gives an expression value of 10-500 arbitrary units). The average of four biological replicates ±s.e.m. was plotted.

Ecdysone titers

Biological replicates of 4-15 larvae were homogenized twice in methanol and cleared by centrifugation to give a final combined volume of ∼360 µl. Duplicate 100 µl samples were dried and resuspended overnight in 50 µl EIA buffer (Cayman Chemical). Cayman Chemical reagents for 20-HE ELISA were used as per manufacturer's recommendation with two changes: in some experiments, the E antibody L2-B (kind gift of Jean-Paul Delbecque, Aquitaine Institute for Cognitive and Integrative Neuroscience, Bordeaux, France) was substituted for the Cayman antiserum, and in other cases where there was a low E titer because of small sample size, the 20-HE AChE tracer was diluted up to 1:5 in the reaction. The standard curve was determined using GraphPad Prism software, non-linear regression curve fit, asymmetric sigmoidal, 5PL, X is log (conc). Per animal, E titers were adjusted for the volume used in the assay.

Acknowledgements
We thank the Bloomington *Drosophila* Stock Center (BDSC) for numerous *Drosophila* lines and Aidan Peterson and Derya Deveci for comments on the manuscript; Colby Starker, Michelle Christian and Dan Voytas for help in designing and making TALENs for the *Ptth* null mutant production; Anna Petryk and Michael Jarcho for producing UAST-*sad*, *phm* and *dib* constructs; and Thomas Phil for technical support.

Competing interests
The authors declare no competing or financial interests.

Author contributions
Conceptualization: M.S., F.A.M., P.L., M.B.O., N.M.R.; Methodology: M.S., P.L., M.B.O., N.M.R.; Formal analysis: M.S., N.M.R.; Investigation: M.S., X.P., F.A.M., A.C.G., N.M.R.; Writing - original draft: M.B.O., N.M.R.; Writing - review & editing: M.S., P.L., M.B.O., N.M.R.; Visualization: M.S., X.P., F.A.M., N.M.R.; Supervision: P.L., M.B.O., N.M.R.; Project administration: M.S., N.M.R.; Funding acquisition: P.L., M.B.O.

Funding
This work was supported by Institut National de la Santé et de la Recherche Médicale (INSERM), Centre National de la Recherche Scientifique (CNRS), Fondation ARC pour la Recherche sur le Cancer grant PGA120150202355 and European Research Council Advanced Grant 268813 to P.L. and N.M.R.; and National Institutes of Health grant R35-GM118029 to M.B.O. F.A.M. is a recipient of Ramon y Cajal Contract RyC-2014-14961 from the Ministerio de Economía y Competitividad and supported by BFU2014-54346-JIN. Deposited in PMC for release after 12 months.

Supplementary information
Supplementary information available online at
http://dev.biologists.org/lookup/doi/10.1242/dev.159699.supplemental

References

Amarnath, S., Stevens, L. M. and Stein, D. S. (2017). Reconstitution of Torso signaling in cultured cells suggests a role for both Trunk and Torso-like in receptor activation. *Development* **144**, 677-686.
Baena-Lopez, L. A., Alexandre, C., Mitchell, A., Pasakarnis, L. and Vincent, J.-P. (2013). Accelerated homologous recombination and subsequent genome modification in *Drosophila*. *Development* **140**, 4818-4825.
Barker, J. S. F. and Podger, R. N. (1970). Interspecific competition between *Drosophila melanogaster* and *Drosophila simulans*: effects of larval density on viability, developmental period and adult body weight. *Ecology* **51**, 170-189.
Bergland, A. O., Genissel, A., Nuzhdin, S. V. and Tatar, M. (2008). Quantitative trait loci affecting phenotypic plasticity and the allometric relationship of ovariole number and thorax length in *Drosophila melanogaster*. *Genetics* **180**, 567-582.
Boulan, L., Martín, D. and Milán, M. (2013). bantam miRNA promotes systemic growth by connecting insulin signaling and ecdysone production. *Curr. Biol.* **23**, 473-478.
Bubli, O. A., Imasheva, A. G. and Loeschcke, V. (1998). Selection for knockdown resistance to heat in *Drosophila Melanogaster* at high and low larval densities. *Evolution* **52**, 619-625.
Caldwell, P. E., Walkiewicz, M. and Stern, M. (2005). Ras activity in the *Drosophila* prothoracic gland regulates body size and developmental rate via ecdysone release. *Curr. Biol.* **15**, 1785-1795.
Casanova, J., Furriols, M., McCormick, C. A. and Struhl, G. (1995). Similarities between trunk and spatzle, putative extracellular ligands specifying body pattern in *Drosophila*. *Genes Dev.* **9**, 2539-2544.
Chippindale, A. K., Leroi, A. M., Kim, S. B. and Rose, M. R. (1993). Phenotypic plasticity and selection in *Drosophila* life-history evolution. 1. Nutrition and the cost of reproduction. *J. Evol. Biol.* **6**, 171-193.
Colombani, J., Bianchini, L., Layalle, S., Pondeville, E., Dauphin-Villemant, C., Antoniewski, C., Carre, C., Noselli, S. and Leopold, P. (2005). Antagonistic actions of ecdysone and insulins determine final size in *Drosophila*. *Science* **310**, 667-670.
Colombani, J., Andersen, D. S., Boulan, L., Boone, E., Romero, N., Virolle, V., Texada, M. and Léopold, P. (2015). *Drosophila* Lgr3 couples organ growth with maturation and ensures developmental stability. *Curr. Biol.* **25**, 2723-2729.
Danielsen, E. T., Moeller, M. E. and Rewitz, K. F. (2013). Nutrient signaling and developmental timing of maturation. *Curr. Top. Dev. Biol.* **105**, 37-67.
Danielsen, E. T., Moeller, M. E., Dorry, E., Komura-Kawa, T., Fujimoto, Y., Troelsen, J. T., Herder, R., O'Connor, M. B., Niwa, R. and Rewitz, K. F. (2014). Transcriptional control of steroid biosynthesis genes in the *Drosophila* prothoracic gland by ventral veins lacking and knirps. *PLoS Genet.* **10**, e1004343.
David, J. R. (1970). Le numbre d'ovarioles chez la avec la fecondite et valeur adaptive. *Arch. Zool. Exp. Genet.* **111**, 357-370.
Deng, H. and Kerppola, T. K. (2013). Regulation of *Drosophila* metamorphosis by xenobiotic response regulators. *PLoS Genet.* **9**, e1003263.
Denver, R. J. (1997). Environmental stress as a developmental cue: corticotropin-releasing hormone is a proximate mediator of adaptive phenotypic plasticity in amphibian metamorphosis. *Horm. Behav.* **31**, 169-179.
Di Cara, F. and King-Jones, K. (2013). How clocks and hormones act in concert to control the timing of insect development. *Curr. Top. Dev. Biol.* **105**, 1-36.
Garelli, A., Heredia, F., Casimiro, A. P., Macedo, A., Nunes, C., Garcez, M., Dias, A. R., Volonte, Y. A., Uhlmann, T., Caparros, E. et al. (2015). Dilp8 requires the neuronal relaxin receptor Lgr3 to couple growth to developmental timing. *Nat. Commun.* **6**, 8732.
Ghosh, A., McBrayer, Z. and O'Connor, M. B. (2010). The *Drosophila* gap gene giant regulates ecdysone production through specification of the PTTH-producing neurons. *Dev. Biol.* **347**, 271-278.
Gibbens, Y. Y., Warren, J. T., Gilbert, L. I. and O'Connor, M. B. (2011). Neuroendocrine regulation of *Drosophila* metamorphosis requires TGFbeta/Activin signaling. *Development* **138**, 2693-2703.
Gloor, G. B., Preston, C. R., Johnson-Schlitz, D. M., Nassif, N. A., Phillis, R. W., Benz, W. K., Robertson, H. M. and Engels, W. R. (1993). Type I repressors of P element mobility. *Genetics* **135**, 81-95.
Gokhale, R. H., Hayashi, T., Mirque, C. D. and Shingleton, A. W. (2016). Intra-organ growth coordination in *Drosophila* is mediated by systemic ecdysone signaling. *Dev. Biol.* **418**, 135-145.
Gotthard, K. and Nylin, S. (1995). Adaptive plasticity and plasticity as an adaptation: a selective review of plasticity in animal morphology and life-history. *Oikos* **74**, 3-17.
Hackney, J. F., Zolali-Meybodi, O. and Cherbas, P. (2012). Tissue damage disrupts developmental progression and ecdysteroid biosynthesis in *Drosophila*. *PLoS ONE* **7**, e49105.
Hamada, F. N., Rosenzweig, M., Kang, K., Pulver, S. R., Ghezzi, A., Jegla, T. J. and Garrity, P. A. (2008). An internal thermal sensor controlling temperature preference in *Drosophila*. *Nature* **454**, 217-220.
Herboso, L., Oliveira, M. M., Talamillo, A., Perez, C., Gonzalez, M., Martin, D., Sutherland, J. D., Shingleton, A. W., Mirth, C. K. and Barrio, R. (2015). Ecdysone promotes growth of imaginal discs through the regulation of Thor in *D. melanogaster*. *Sci. Rep.* **5**, 12383.
Hock, T., Cottrill, T., Keegan, J. and Garza, D. (2000). The E23 early gene of *Drosophila* encodes an ecdysone-inducible ATP-binding cassette transporter capable of repressing ecdysone-mediated gene activation. *Proc. Natl. Acad. Sci. USA* **97**, 9519-9524.
Hodge, J. J. (2009). Ion channels to inactivate neurons in *Drosophila*. *Front. Mol. Neurosci.* **2**, 13.
Horvath, B. and Kalinka, A. T. (2016). Effects of larval crowding on quantitative variation for development time and viability in *Drosophila melanogaster*. *Ecol. Evol.* **6**, 8460-8473.
Jaszczak, J. S., Wolpe, J. B., Bhandari, R., Jaszczak, R. G. and Halme, A. (2016). Growth coordination during *Drosophila melanogaster* imaginal disc regeneration is mediated by signaling through the relaxin receptor Lgr3 in the prothoracic gland. *Genetics* **204**, 703-709.
Jenni, S., Goyal, Y., von Grotthuss, M., Shvartsman, S. Y. and Klein, D. E. (2015). Structural basis of neurohormone perception by the receptor tyrosine kinase Torso. *Mol. Cell* **60**, 941-952.
Joshi, A., Knight, C. D. and Mueller, L. D. (1996a). Genetics of larval urea tolerance in *Drosophila melanogaster*. *Heredity* **77**, 33-39.
Joshi, A., Shiotsugu, J. and Mueller, L. D. (1996b). Phenotypic enhancement of longevity by environmental urea in *Drosophila melanogaster*. *Exp. Gerontol.* **31**, 533-544.
Jun, J. W., Han, G., Yun, H. M., Lee, G. J. and Hyun, S. (2016). Torso, a *Drosophila* receptor tyrosine kinase, plays a novel role in the larval fat body in regulating insulin signaling and body growth. *J. Comp. Physiol. B* **186**, 701-709.
Kataoka, H., Nagasawa, H., Isogai, A., Ishizaki, H. and Suzuki, A. (1991). Prothoracicotropic hormone of the silkworm, Bombyx mori: amino acid sequence and dimeric structure. *Agric. Biol. Chem.* **55**, 73-86.
Kawakami, A., Kataoka, H., Oka, T., Mizoguchi, A., Kimura-Kawakami, M., Adachi, T., Iwami, M., Nagasawa, H., Suzuki, A. and Ishizaki, H. (1990). Molecular cloning of the Bombyx mori prothoracicotropic hormone. *Science* **247**, 1333-1335.
Keightley, D. A., Lou, K. J. and Smith, W. A. (1990). Involvement of translation and transcription in insect steroidogenesis. *Mol. Cell. Endocrinol.* **74**, 229-237.
Kolss, M., Vijendravarma, R. K., Schwaller, G. and Kawecki, T. J. (2009). Life-history consequences of adaptation to larval nutritional stress in *Drosophila*. *Evolution* **63**, 2389-2401.
Komura-Kawa, T., Hirota, K., Shimada-Niwa, Y., Yamauchi, R., Shimell, M., Shinoda, T., Fukamizu, A., O'Connor, M. B. and Niwa, R. (2015). The *Drosophila* zinc finger transcription factor Ouija board controls ecdysteroid biosynthesis through specific regulation of spookier. *PLoS Genet.* **11**, e1005712.
Konogami, T., Yang, Y., Ogihara, M. H., Hikiba, J., Kataoka, H. and Saito, K. (2016). Ligand-dependent responses of the silkworm prothoracicotropic hormone receptor, Torso, are maintained by unusual intermolecular disulfide bridges in the transmembrane region. *Sci. Rep.* **6**, 22437.

Kopec, S. (1922). Studies on the necessity of the brain for the inception of insect metamorphosis. *Biol. Bull.* **42**, 323-342.
Kouser, S., Palaksha, S. and Shakunthala, V. (2013). Study on fitness of *Drosophila melanogaster* in different light regimes. *Biol. Rhythm. Res.* **45**, 293-300.
Koyama, T., Rodrigues, M. A., Athanasiadis, A., Shingleton, A. W. and Mirth, C. K. (2014). Nutritional control of body size through FoxO-Ultraspiracle mediated ecdysone biosynthesis. *Elife* **3**, e03091.
Kulesza, P., Lee, C.-Y. and Watson, R. D. (1994). Protein synthesis and ecdysteroidogenesis in prothoracic glands of the tobacco hornworm (Manduca sexta): stimulation by big prothoracicotropic hormone. *Gen. Comp. Endocrinol.* **93**, 448-458.
Lafont, R., Dauphin-Villemant, C. and Warren, J. T. (2005). Ecdysteroid chemistry and biochemistry. In *Comprehensive Molecular Insect Sciences* (ed. L. I. Gilbert, K. Iatrou and S. Gill), pp. 125-195. Oxford: Elsevier.
Lavalle, S., Arquier, N. and Léopold, P. (2008). The Tor pathway couples nutrition and developmental timing in *Drosophila*. *Dev. Cell* **15**, 568-577.
Lessells, C. M. (2008). Neuroendocrine control of life histories: what do we need to know to understand the evolution of phenotypic plasticity? *Philos. Trans. R. Soc. Lond. B Biol. Sci.* **363**, 1589-1598.
Mast, J. D., De Moraes, C. M., Alborn, H. T., Lavis, L. D. and Stern, D. L. (2014). Evolved differences in larval social behavior mediated by novel pheromones. *Elife* **3**, e04205.
May, C. M., Doroszuk, A. and Zwaan, B. J. (2015). The effect of developmental nutrition on life span and fecundity depends on the adult reproductive environment in *Drosophila melanogaster*. *Ecol. Evol.* **5**, 1156-1168.
McBrayer, Z., Ono, H., Shimell, M., Parvy, J.-P., Beckstead, R. B., Warren, J. T., Thummel, C. S., Dauphin-Villemant, C., Gilbert, L. I. and O'Connor, M. B. (2007). Prothoracicotropic hormone regulates developmental timing and body size in *Drosophila*. *Dev. Cell* **13**, 857-871.
Mendes, C. C. and Mirth, C. K. (2016). Stage-specific plasticity in ovary size is regulated by insulin/insulin-like growth factor and ecdysone signaling in *Drosophila*. *Genetics* **202**, 703-719.
Miller, R. S. and Thomas, J. L. (1958). The effects of larval crowding and body size on the longevity of adult *Drosophila melanogaster*. *Ecology* **39**, 118-125.
Mirth, C. K. and Riddiford, L. M. (2007). Size assessment and growth control: how adult size is determined in insects. *BioEssays* **29**, 344-355.
Mirth, C. K. and Shingleton, A. W. (2012). Integrating body and organ size in *Drosophila*: recent advances and outstanding problems. *Front. Endocrinol.* **3**, 49.
Mirth, C., Truman, J. W. and Riddiford, L. M. (2005). The role of the prothoracic gland in determining critical weight for metamorphosis in *Drosophila melanogaster*. *Curr. Biol.* **15**, 1796-1807.
Moeller, M. E., Danielsen, E. T., Herder, R., O'Connor, M. B. and Rewitz, K. F. (2013). Dynamic feedback circuits function as a switch for shaping a maturation-inducing steroid pulse in *Drosophila*. *Development* **140**, 4730-4739.
Moeller, M. E., Nagy, S., Gerlach, S. U., Soegaard, K. C., Danielsen, E. T., Texada, M. J. and Rewitz, K. F. (2017). Warts signaling controls organ and body growth through regulation of ecdysone. *Curr. Biol.* **27**, 1652-1659.e4.
Nijhout, H. F., Riddiford, L. M., Mirth, C., Shingleton, A. W., Suzuki, Y. and Callier, V. (2014). The developmental control of size in insects. *Wiley Interdiscip. Rev. Dev. Biol.* **3**, 113-134.
Niwa, R., Sakudoh, T., Namiki, T., Saida, K., Fujimoto, Y. and Kataoka, H. (2005). The ecdysteroidogenic P450 Cyp302a1/disembodied from the silkworm, Bombyx mori, is transcriptionally regulated by prothoracicotropic hormone. *Insect Mol. Biol.* **14**, 563-571.
Niwa, R., Namiki, T., Ito, K., Shimada-Niwa, Y., Kiuchi, M., Kawaoka, S., Kayukawa, T., Banno, Y., Fujimoto, Y., Shigenobu, S. et al. (2010). Non-molting glossy/shroud encodes a short-chain dehydrogenase/reductase that functions in the 'Black Box' of the ecdysteroid biosynthesis pathway. *Development* **137**, 1991-1999.
Noguti, T., Adachi-Yamada, T., Katagiri, T., Kawakami, A., Iwami, M., Ishibashi, J., Kataoka, H., Suzuki, A., G□, M. and Ishizaki, H. (1995). Insect prothoracicotropic hormone: a new member of the vertebrate growth factor superfamily. *FEBS Lett.* **376**, 251-256.
Ohhara, Y., Kobayashi, S. and Yamanaka, N. (2017). Nutrient-dependent endocycling in steroidogenic tissue dictates timing of metamorphosis in *Drosophila melanogaster*. *PLoS Genet.* **13**, e1006583.
Ou, Q., Magico, A. and King-Jones, K. (2011). Nuclear receptor DHR4 controls the timing of steroid hormone pulses during *Drosophila* development. *PLoS Biol.* **9**, e1001160.
Parker, N. F. and Shingleton, A. W. (2011). The coordination of growth among *Drosophila* organs in response to localized growth-perturbation. *Dev. Biol.* **357**, 318-325.
Parvy, J.-P., Blais, C., Bernard, F., Warren, J. T., Petryk, A., Gilbert, L. I., O'Connor, M., B. and Dauphin-Villemant, C. (2005). A role for betaFTZ-F1 in regulating ecdysteroid titers during post-embryonic development in *Drosophila melanogaster*. *Dev. Biol.* **282**, 84-94.
Popoff, M. R. and Poulain, B. (2010). Bacterial toxins and the nervous system: neurotoxins and multipotential toxins interacting with neuronal cells. *Toxins* **2**, 683-737.
Prout, T. and Mcchesney, F. (1985). Competition among immatures affects their adult fertility: population dynamics. *Am. Nat.* **126**, 521-558.
Rewitz, K. F. and O'Connor, M. B. (2011). Timing is everything: PTTH mediated DHR4 nucleocytoplasmic trafficking sets the tempo of *Drosophila* steroid production. *Front. Endocrinol.* **2**, 108.
Rewitz, K. F., Yamanaka, N., Gilbert, L. I. and O'Connor, M. B. (2009). The insect neuropeptide PTTH activates receptor tyrosine kinase torso to initiate metamorphosis. *Science* **326**, 1403-1405.
Rewitz, K. F., Yamanaka, N. and O'Connor, M. B. (2013). Developmental checkpoints and feedback circuits time insect maturation. *Curr. Top. Dev. Biol.* **103**, 1-33.
Rodrigues, M. A., Martins, N. E., Balancé, L. F., Broom, L. N., Dias, A. J. S., Fernandes, A. S. D., Rodrigues, F., Sucena, E. and Mirth, C. K. (2015). *Drosophila melanogaster* larvae make nutritional choices that minimize developmental time. *J. Insect Physiol.* **81**, 69-80.
Rybczynski, R. and Gilbert, L. I. (1995). Prothoracicotropic hormone elicits a rapid, developmentally specific synthesis of beta tubulin in an insect endocrine gland. *Dev. Biol.* **169**, 15-28.
Schering, J. F., Davis, D. G., Ranashinghe, A. and Teeare, C. A. (1984). Effects of larval crowding on life history parameters in *Drosophila melanogaster*. *Exp. Gerentol.* **77**, 329-332.
Selcho, M., Millán, C., Palacios-Muñoz, A., Ruf, F., Ubillo, L., Chen, J., Bergmann, G., Ito, C., Silva, V., Wegener, C. et al. (2017). Central and peripheral clocks are coupled by a neuropeptide pathway in *Drosophila*. *Nat. Commun.* **8**, 15563.
Shimada-Niwa, Y. and Niwa, R. (2014). Serotonergic neurons respond to nutrients and regulate the timing of steroid hormone biosynthesis in *Drosophila*. *Nat. Commun.* **5**, 5778.
Shingleton, A. W., Frankino, W. A., Flatt, T., Nijhout, H. F. and Emlen, D. J. (2007). Size and shape: the developmental regulation of static allometry in insects. *BioEssays* **29**, 536-548.
Siegmund, T. and Korge, G. (2001). Innervation of the ring gland of *Drosophila melanogaster*. *J. Comp. Neurol.* **431**, 481-491.
Stieper, B. C., Kupershtok, M., Driscoll, M. V. and Shingleton, A. W. (2008). Imaginal discs regulate developmental timing in *Drosophila melanogaster*. *Dev. Biol.* **321**, 18-26.
Tennessen, J. M. and Thummel, C. S. (2011). Coordinating growth and maturation – insights from *Drosophila*. *Curr. Biol.* **21**, R750-R757.
Uchibori-Asano, M., Kayukawa, T., Sezutsu, H., Shinoda, T. and Daimon, T. (2017). Severe developmental timing defects in the prothoracicotropic hormone (PTTH)-deficient silkworm, Bombyx mori. *Insect Biochem. Mol. Biol.* **87**, 14-25.
Vallejo, D. M., Juarez-Carreño, S., Bolivar, J., Morante, J. and Dominguez, M. (2015). A brain circuit that synchronizes growth and maturation revealed through Dilp8 binding to Lgr3. *Science* **350**, aac6767.
Walkiewicz, M. A. and Stern, M. (2009). Increased insulin/insulin growth factor signaling advances the onset of metamorphosis in *Drosophila*. *PLoS ONE* **4**, e5072.
Warren, J. T., Yerushalmi, Y., Shimell, M. J., O'Connor, M. B., Restifo, L. L. and Gilbert, L. I. (2006). Discrete pulses of molting hormone, 20-hydroxyecdysone, during late larval development of *Drosophila melanogaster*: correlations with changes in gene activity. *Dev. Dyn.* **235**, 315-326.
Williams, C. M. (1952). Physiology of insect diapause. IV. The brain and prothoracic glands as an endocrine system in the Cecropia Silkworm. *Biol. Bull.* **103**, 120-138.
Yamanaka, N., Rewitz, K. F. and O'Connor, M. B. (2013a). Ecdysone control of developmental transitions: lessons from *Drosophila* research. *Annu. Rev. Entomol.* **58**, 497-516.
Yamanaka, N., Romero, N. M., Martin, F. A., Rewitz, K. F., Sun, M., O'Connor, M. B. and Leopold, P. (2013b). Neuroendocrine control of *Drosophila* larval light preference. *Science* **341**, 1113-1116.
Yamanaka, N., Marqués, G. and O'Connor, M. B. (2015). Vesicle-mediated steroid hormone secretion in *Drosophila melanogaster*. *Cell* **163**, 907-919.
Yoshiyama, T., Namiki, T., Mita, K., Kataoka, H. and Niwa, R. (2006). Neverland is an evolutionally conserved Rieske-domain protein that is essential for ecdysone synthesis and insect growth. *Development* **133**, 2565-2574.